NJC

Accepted Manuscript

This is an *Accepted Manuscript*, which has been through the Royal Society of Chemistry peer review process and has been accepted for publication.

Accepted Manuscripts are published online shortly after acceptance, before technical editing, formatting and proof reading. Using this free service, authors can make their results available to the community, in citable form, before we publish the edited article. We will replace this *Accepted Manuscript* with the edited and formatted *Advance Article* as soon as it is available.

You can find more information about *Accepted Manuscripts* in the Information for Authors.

Please note that technical editing may introduce minor changes to the text and/or graphics, which may alter content. The journal's standard Terms & Conditions and the Ethical guidelines still apply. In no event shall the Royal Society of Chemistry be held responsible for any errors or omissions in this *Accepted Manuscript* or any consequences arising from the use of any information it contains.

ROYAL SOCIETY OF CHEMISTRY

www.rsc.org/njc

Graphical Abstract

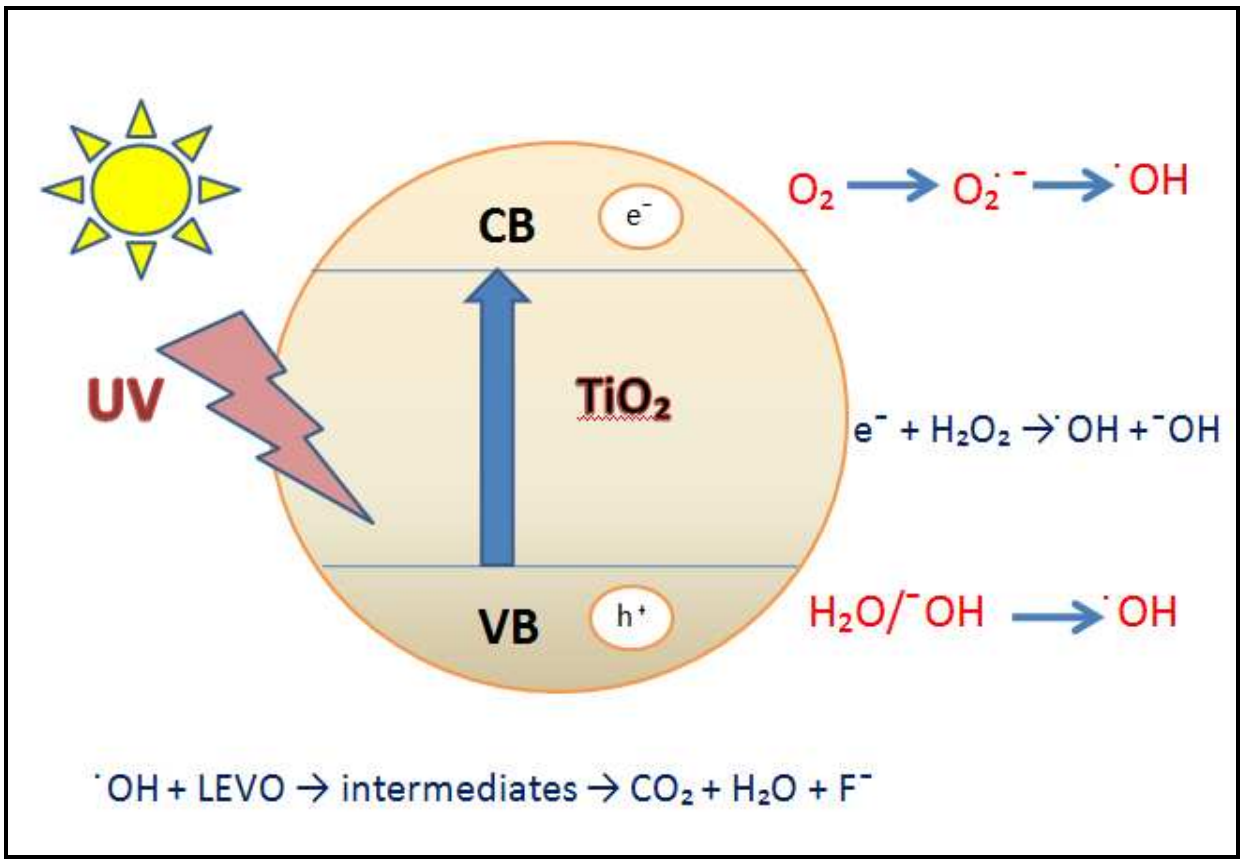

Photocatalytic degradation of antibiotic levofloxacin using well-crystalline TiO_2 nanoparticles

Sushil Kumar Kansal[1*], Pranati Kundu[1], Swati Sood[2], Randeep Lamba[2], Ahmad Umar[3,4]*, S.K.Mehta[2]

[1]Dr. S.S. Bhatnagar University Institute of Chemical Engineering & Technology, Panjab University, Chandigarh-160014, India

[2]Department of Chemistry, Panjab University, Chandigarh-160014, India

[3]Department of Chemistry, College of Science and Arts, Najran University, P.O.Box-1988, Najran-11001, Kingdom of Saudi Arabia

[4]Promising Centre for Sensors and Electronic Devices (PCSED), Najran University, P.O.Box-1988, Najran-11001, Kingdom of Saudi Arabia

***Corresponding authors:**

E-mail Address: sushilkk1@pu.ac.in, sushilkk1@yahoo.co.in (S. K. Kansal)

ahmadumar786@gmail.com (Ahmad Umar)

Graphical abstract

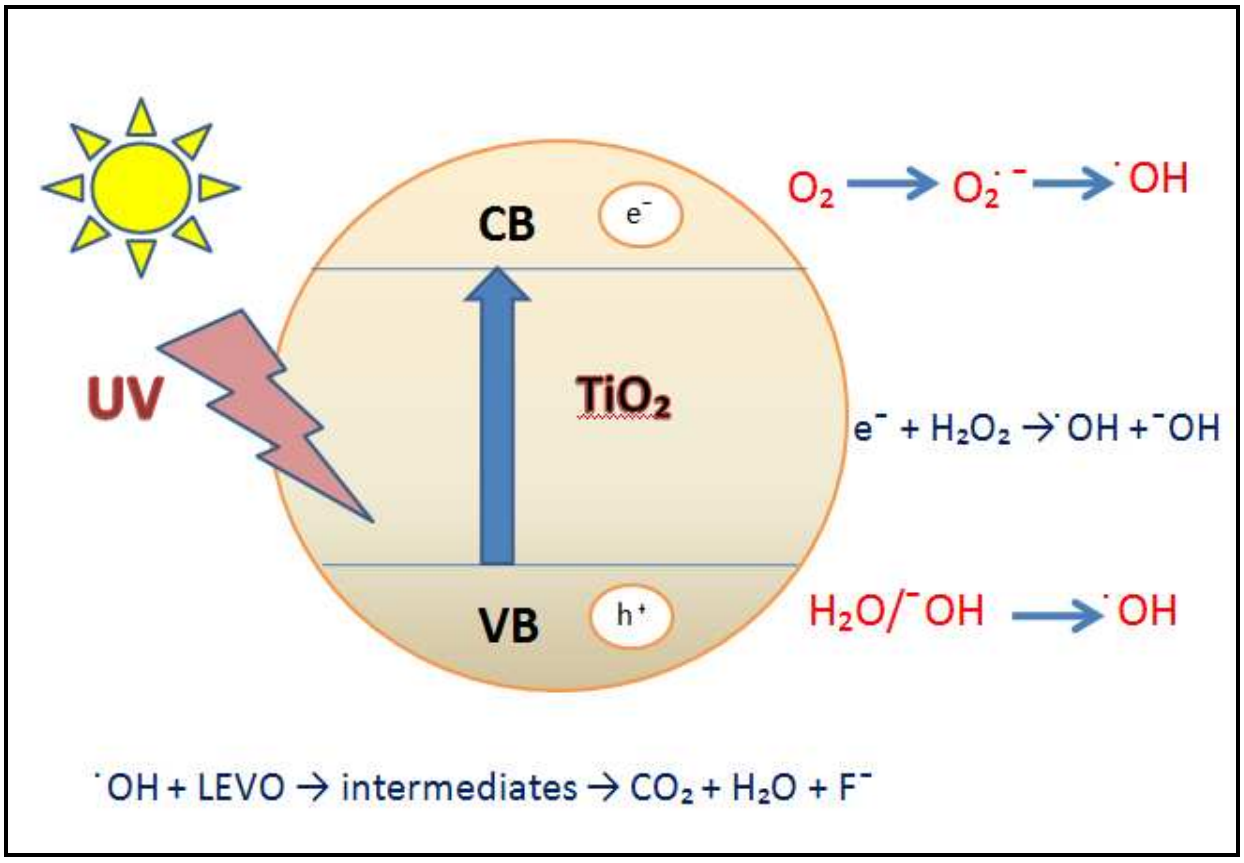

Highly crystalline TiO_2 (anatase) nanoparticles were synthesized by facile sol-gel method for photocatalytic degradation and antibacterial activity of commonly used antibiotic drug, levofloxacin.

Abstract

This paper reports the photocatalytic degradation of levofloxacin (LEVO), a widely used antibiotic drug, using well-crystalline TiO_2 nanoparticles. The TiO_2 nanoparticles were synthesized using sol-gel technique and characterized by various techniques in terms of their morphological, structural, compositional, thermal and optical properties. The detailed studies revealed that the prepared TiO_2 nanoparticles are grown in high-density, possessing well-crystallinity and exhibiting good optical properties. Over 90% photocatalytic degradation of LEVO was achieved by prepared TiO_2 nanoparticles in 120 min under UV light illumination. By comparing the photocatalytic degradation properties of prepared TiO_2 nanoparticles with commercially available TiO_2 catalyst (P 25 and PC-50), it was observed that the as-synthesized TiO_2 nanoparticles exhibited superior photocatalytic performance towards LEVO. Moreover, the antibiotic efficacy of levofloxacin was also performed against *E.coli* and interestingly it was found that the antibacterial activity was drastically inhibited after the treatment of drug solutions with prepared photocatalyst.

Keywords: TiO_2 nanoparticles, Levofloxacin (LEVO), Sol-gel technique, *E. coli*

1. Introduction

Availability of large number of healthcare products such as antibiotics, analgesics, anti-inflammatories, hypnotics, etc. for human beings has improved the life quality in general. However due to the excretion of these drugs and their metabolites by humans and animals, they ultimately accumulate in waste water [1-14]. The presence of such pharmaceuticals in the aquatic environment is of global concern as their long term presence can affect the aquatic organisms even in low concentration and increase the population of antibiotic resistant pathogens in waste water [15-17]. Levofloxacin (LEVO) i.e chiral fluorinated carboxyquinolone, is a broad spectrum antibiotic that belongs to fluoroquinolone class and is known for its broad spectrum activity against gram positive bacteria (*Staphylococcus aureus, Streptococcus pneumoniae, Staphylococcus epidermidis*) and gram negative bacteria (*Escherichia coli, Haemophilus influenzae, Klebsiella pneumoniae*) [16-18]. In addition to this, it has an excellent tissue penetration and is available in both oral and intravenous formulations. However, it may produce serious and life threatening adverse reactions. According to the U.S Food and Drug Administration (FDA), the LEVO may cause worsening of myasthenia gravis symptoms, including muscle weakness and breathing problems as well as spontaneous tendon ruptures. Due to these, it is important to propose an efficient treatment method which can transform this antibiotic to non-toxic and biodegradable species. In this regard, various conventional methods have been proposed in the literature for the degradation of LEVO, however, these methods were been found to be ineffective for the complete mineralization due to its low biodegradability. Hence, there is a considerable need for the efficient degradation of this harmful and widely used drug by exploring other potential technologies.

Recently, various advanced oxidation processes (AOP) have received great attention in the degradation of such compounds. Different types of AOPs include ozonation [19-21], Fenton and Photo Fenton oxidation [22], Photolysis and H_2O_2 enhanced photolysis [23, 24], heterogeneous photocatalysis [25, 26], sonolysis [27], etc. Among these AOPs, semiconductor photocatalysis using different metal oxides/sulfides (TiO_2, ZnO, ZnS, Fe_2O_3, CdS, WO_3, graphene based metal oxides, etc.) is one of the most promising techniques for the complete degradation of organic compounds [28-42].

Among various heterogeneous semiconductor photocatalysts, TiO_2 possesses a special place due to its own properties such as its inertness, long term stability, non-toxicity, low-cost synthesis and easy recovery by filtration and centrifugation methods, wide band gap (E_{bg}=3.2 eV for anatase phase) and several other excellent properties [43, 44]. Due to these afore mentioned properties, TiO_2 has been widely used for effective photocatalytic degradation of various dyes and other organic pollutants [45- 48].

In the present study, TiO_2 nanoparticles were synthesized by simple sol-gel method and characterized by various techniques. Moreover, the photocatalytic activity of the prepared TiO_2 nanoparticles was evaluated for the degradation of LEVO, a model antibiotic compound, under UV light illumination. Furthermore, the antibacterial activity of the drug against *E. coli* was also evaluated before and after its photo-degradation.

2. Experimental details

2.1. *Reagents and Materials*

Methanol and Titanium isopropoxide (IV) of analytical grades were purchased from Merck. Trypton, yeast extract and sodium chloride were purchased from Himedia. *E.coli* culture

was obtained from Institute of Microbial Technology. LEVO was gifted by Sourabh Chemicals, Derabassi, Chandigarh, India. All the chemicals were used as received without further purification.

2.2. Synthesis of TiO_2 nanoparticles

TiO_2 nanoparticles were synthesized by sol-gel method using titanium isopropoxide (IV) as a precursor. In a typical synthesis procedure, 3.7 mL of titanium isopropoxide (IV) was added to 40 mL of methanol. To this reaction mixture 20 mL of water and 40 mL of methanol was added. This was further kept under continuous and vigorous stirring at 60 °C. The vigorous stirring was continued at the same temperature until the white precipitate was obtained. The obtained precipitate was then dried at 40 ºC and grounded using mortar and pestle to obtain fine TiO_2 powder. Finally, the synthesized powder was calcined at 400 ºC for 2 h to obtain desired TiO_2 nanoparticles which were characterized in detail in terms of their morphological, structural, optical, thermal and photocatalytic properties.

2.3. Characterization

The prepared samples were characterized by various techniques. The general morphologies of as-prepared nanoparticles were examined by transmission electron microscopy (TEM; FEI Tecnai G2 F20), equipped with EDAAX. The crystallinity and phase identification of the prepared nanoparticles were examined by X-ray diffraction (XRD; Panalytical Model X'Pert PRO) using Cu-Kα radiation (k = 1.54056 Å) at 45 kV and 40 mA in the range of 2θ = 10-80°. The chemical composition and purity of prepared nanoparticles were examined by Fourier transform infrared (FTIR) spectroscopy using KBr as reference in the range of 500-4000 cm^{-1}.

Thermogravimetric analysis (TGA) was mapped in the temperature range of 0°-1000 °C with the acceleration speed of 10 ^{0}C min^{-1} using TGA/DSC analyzer (Perkin-Elmer STA 6000 simultaneous thermal analyzer). The optical property of prepared nanoparticles was examined by room-temperature photoluminescence (PL) in the range of 300-550 nm at excitation wavelength of 290 nm on Perkin-Elmer LS-55 fluorescence spectrophotometer.

2.4. Photocatalytic Experiment

The photocatalytic degradation of LEVO was carried out in a UV chamber equipped with seven 18W UV tubes (Philips, 365 nm wavelength) in a specially designed double walled reaction vessel (volume 500 mL). The intensity of the UV light was measured by UVA light meter (Model UVA-365, Lutron) and found to be 0.5 mW/cm^2. The catalyst was immersed into 100 mL aqueous solution of LEVO (25 mg/L) and the solution was magnetically stirred in dark for 30 min to establish the adsoption/desorption equilibrium. Then the solution was illuminated under UV light. The aliquot was taken out with a syringe after illumination at different time intervals and filtered through Millipore syringe filter of 0.45 μm. The absorption spectra of the dye solutions were recorded using Systronics-2202 spectrometer and the rate of degradation was observed in terms of change in intensity at λ_{max} of the dye. The degradation efficiency (%) has been calculated as:

$$\textbf{\% Degradation} = (C_0\text{-}C)/C_0 \times 100$$

Where, C_0 is the initial concentration of dye and C is the concentration of dye after photo-irradiation

2.5. Antimicrobial activity test

E. coli was grown in Luria Bertani agar (LBA) plates. The LBA medium contained 5 g yeast extract, 5 g NaCl, 10 g tryptone and 15 g agar in 1 L distilled water. The LBA medium was then sterilized in an autoclave for 15 min at 121°C and 15 lb pressure. After cooling, it was poured in the sterile petri dishes placed in laminar flow chamber and allowed to solidify. The suspension of *E. coli* culture was prepared in sterilized distilled water. Cell suspension (100 µL) was then transferred to the LBA medium plates and spread with the help of glass spreader. Small wells were made in inoculated LBA plates and 20 µL of irradiated samples were transferred to the wells carefully. The plates were then incubated at 37 °C for 24 h and the zones of growth inhibition of *E. coli* around the wells were measured in mm. Pure solution of the antibiotic was used as positive control.

3. Results and Discussion

3.1. Characterization of prepared TiO_2 nanoparticles

To examine the general morphologies, the as-prepared TiO_2 materials were characterized by using TEM. Figure 1 (a) exhibits the typical TEM image which confirmed that the prepared TiO_2 products are nanoparticles that are grown in large quantity and possessing almost spherical shape. The sizes of the nanoparticles are in the range of ~20 ± 5 nm. Moreover, due to high density growth agglomeration in the nanoparticles has been observed. The detailed morphological properties of as-prepared TiO_2 nanoparticles were examined by high resolution TEM (HRTEM) and the obtained result is shown in figure 1 (b). The observed HRTEM image shows a very clear and well-defined lattice fringes with the lattice spacing of ~0.35 nm, which is fully consistent with the distance of (101) crystalline plane of the anatase TiO_2. To examine the

elemental compositions, the as-prepared TiO_2 nanoparticles were examined by energy dispersive spectroscopy (EDS) attached with TEM and observed result is shown in figure 1(c). The observed EDS spectrum confirms that the prepared nanoparticles are made of Ti and Oxygen. The presence of Cu peaks in the EDS spectrum was due to copper grid which was used during the measurement.

The crystallinity and crystal phases of prepared TiO_2 nanoparticles were examined by X-ray diffraction (XRD). Figure 1 (d) shows the typical XRD patterns of prepared TiO_2 nanoparticles. The peaks located at 2θ= 25.56, 38.02, 48.3, 54.14, 55.27, 62.69, 68.9, 70.52 and 75.22 were assigned to (101), (004), (200), (105), (211), (204), (116), (220) and (107), respectively which correspond to the anatase phase of TiO_2. The crystalline size of the prepared TiO_2 was determined from the X-ray broadening method using the Scherrer's equation, $D=0.9\lambda/\beta\cos\theta$, where λ is the wavelength of Cu-kα radiation, β is the full width at half maximum intensity and θ is the angle obtained from 2θ value corresponding to the (101) peak attributed to the anatase TiO_2. According to the Scherrer's equation, the calculated average crystalline size was found to be ~17 nm.

The chemical compositions of the prepared TiO_2 nanoparticles were examined by FTIR spectroscopy. Figure 2 (a) depicts the typical FTIR spectrum of prepared TiO_2 nanoparticles. The broad peak located at 670 cm^{-1} corresponds to Ti-O stretching [49]. The appearance of a short peak at 3737 cm^{-1} is related with the OH^- group [50]. The peaks originated at 2919 cm^{-1} and 2851 cm^{-1} correspond to asymmetric and symmetric C-H stretching. Presence of sharp peaks located at 1624 cm^{-1} and 1018 cm^{-1} are corresponding to C=O stretching and plane bending vibration of C-H mode, respectively.

The optical properties of prepared TiO_2 nanoparticles were examined by room-temperature photoluminescence (PL) spectroscopy. Figure 2 (b) exhibits the typical room-temperature PL spectrum of prepared TiO_2 nanoparticles. The obtained PL spectrum exhibited a well-defined, significant emission peak at ~389 nm which is originated due to the band edge free excitons [51]. For comparison, the photoluminescence (PL) properties of commercially available P25 and PC-50 were also examined. The observed PL spectra of P25 and PC-50 are shown in figure S1 (supporting information). For both the materials, the characteristic PL emission peaks appear at ~400 nm which are in good agreement with those reported in the literature [52-53].

To investigate the thermal behavior, the prepared TiO_2 nanoparticles were examined by TGA and DSC analysis. Figure 3 shows the TGA and DSC curve for the prepared TiO_2 nanoparticles. The observed weight loss from 20^0 to 100 ^{0}C was about 2.245%, which is due to water volatilization, also confirmed by endothermic desorption of DSC curve at 290 ^{0}C. From 100^0 to 650°C, the weight loss was about 2.921%, which is attributed to the evaporation of physically absorbed water. The DSC curve shows a strong exothermic peak at 360 °C which is due to the oxidation of organic phase. The observed DSC/TGA results are consistent with the reported literature [54-56].

3.2. Evaluation of photocatalytic activity

The photocatalytic degradation of LEVO was done under UV-illumination using TiO_2 nanoparticles as efficient photocatalyst. The photocatalytic degradation was evaluated by measuring the absorbance on particular wavelength (286.4 nm) at regular time intervals under UV-illumination. The rate of degradation was observed in terms of change in intensity at λ_{max} = 286.4 nm. Figure 4 (a) shows significant decrease in the absorption intensity of LEVO with

increase in the UV irradiation time indicating decrease in the concentration in the presence of TiO_2 nanoparticles. It has also been observed that a new peak arises at wavelength 329.6 nm with increase in irradiation time. This may be attributed to the formation of different intermediates during degradation process which further diminishes with irradiation time. However, when the photo-degradation experiment was conducted in the absence of TiO_2 nanoparticles, no LEVO degradation was detected (UV irradiation alone). Also, in order to investigate the adsorption of LEVO molecules on TiO_2 catalyst, experiments were conducted in dark and it was found that no significant degradation (only about 14%) was observed in 120 minutes (Figure 4 (b)). Three trials of each experiment were performed. The error bars are shown in Figure 4 (b) with the mean standard error of ± 0.0492 min^{-1}.

In order to compare the photocatalytic efficiency of prepared TiO_2 nanoparticles with commercially available TiO_2 (PC-50) photocatalyst, various experiments have been performed by keeping all the reaction conditions same as previous photocatalytic degradation experiments (conc = 25 mg/L, pH= 6, catalyst dose= 1g/L, time = 120 min). Figure 5 (a) exhibits the bar diagram of the obtained experimental results for the photocatalytic degradation of LEVO using prepared TiO_2 nanoparticles and commercially available TiO_2 (PC-50 and P25). Interestingly, it was seen that the prepared TiO_2 nanoparticles exhibited better photocatalytic behavior toward LEVO compared to commercially available photocatalyst. The photocatalytic degradation of LEVO in 120 min with prepared TiO_2 nanoparticles is 90% whereas 78% and 80% was observed with that of commercially available TiO_2 (PC-50) and TiO_2 (P25), respectively. The recyclability of the prepared TiO_2 nanoparticles was also tested by conducting photocatalytic experiments under similar conditions. The photodegradation rate observed for LEVO after second and third cycle was about 82% and 75% respectively, which reflects that the prepared nanoparticles

possess significant catalytic property even after reusing third time, as shown in Fig. 5 (b). The high photocatalytic degradation efficiency of synthesized TiO_2 nanoparticles can be correlated with the small particle size, high anatase content and excellent crystallinity.

The photocatalytic activity of the prepared TiO_2 nanoparticles was evaluated by photo-degradation of the aqueous solution of LEVO under UV irradiation. Figure 6 shows the plausible mechanism for the photocatalytic degradation of LEVO using TiO_2 nanoparticles. The initial step in TiO_2-mediated photocatalysis degradation involves the generation of an (e−/h+) pair, leading to the formation of hydroxyl radicals (•OH) and superoxide radical anions (O_2□ □) as shown below [57-59]. The reaction of HO• with organic pollutants is the most important step that leads to the mineralization of organic pollutants.

$TiO_2 + h\upsilon \rightarrow TiO_2$ (e □ + h^+) (1)

O_2 + e □ → □O_2□ (2)

□O_2□ + h^+ → □HO_2

(3)

2 □$HO_2 \rightarrow O_2 + H_2O_2$

(4)

H_2O_2 + e □ → OH □ + OH □

(5)

□OH + LEVO → intermediates → $CO_2 + H_2O$ + F □

(6)

The organic pollutants are attacked and oxidized by the radicals formed through the above mechanisms and leads the photocatalytic degradation of organic species.

3.3. Evaluation of antibacterial activity

The degradation of LEVO was further confirmed by studying its antibacterial activity against *E.coli* culture. Bioassays were performed on *E.coli* culture inoculated on agar plates by spread-plate method. The effect of photocatalysis on residual antibacterial activity of the irradiated samples was determined by measuring the diameter of *E. coli* inhibition zone around the micro drops (25 μL) sample of treated water on the agar plate. It was observed that with increase in irradiation time, there was a gradual decrease in antibacterial activity of the treated samples. In the control samples, maximum zone of inhibition was observed to be 29 mm. After an interval of 5, 10, 15, 25, 40 and 60 min UV treatment, the zone of inhibition observed were 25, 22, 18, 11, 10 and 9 mm, respectively. After 25 min of UV treatment, more than 80% decrease in antibacterial activity of LEVO was observed. However, after 60 min of UV treatment, the antibacterial activity of the LEVO was found to be negligible. Figure 7 shows the plot of inhibition zone diameter against irradiation time where the curve represents the decrease in antibacterial activity of the LEVO. The end point at the curve shows minimum inhibition zone. The complete absence of antibacterial activity was considered only when there is full growth around the well [60]. The dashed line indicates that there might be some antibacterial activity which cannot be measured accurately [17]. The decrease in inhibition zone diameter can also be considered on the photographs of the LBA medium plates shown in Figure S2 (supporting information).

4. Conclusions

In summary, well-crystalline TiO_2 nanoparticles were synthesized using sol-gel technique and characterized by various techniques. The detailed studies revealed that the prepared TiO_2

nanoparticles are grown in high-density, possessing well-crystallinity and exhibiting good optical properties. The prepared TiO_2 nanoparticles were used as potential and efficient photocatalyst for the photocatalytic degradation of levofloxacin (LEVO), a widely known antibiotic drug. Under UV-illumination, the synthesized TiO_2 nanoparticles exhibited 90% degradation of LEVO. By detailed experiments, it was observed that the prepared TiO_2 nanoparticles exhibited better photocatalytic performance compared to the commercially available TiO_2 (PC-50). Furthermore, the antibacterial activity of LEVO against *E. coli* was drastically inhibited when exposed to levofloxacin solutions treated by the prepared photocatalyst over short irradiation time. The obtained results demonstrated that simply synthesized TiO_2 nanoparticles can efficiently be used for the photocatalytic degradation of antibiotics.

Acknowledgements

The authors great acknowledge the financial support received under the UGC (Major Project), Government of India through a project grant F. No. 41-364/2012(SR) and TEQIP-II grant of Dr. S.S. Bhatnagar UICET, Panjab University, Chandigarh. The authors are also thankful to Sourabh Chemicals, Derabassi, Chandigarh for providing drug samples. Sincere thanks to Prof. Emeritus K. Chaudhary, Department of Microbiology, Maharshi Dayanand University, Rohtak for her help to carry antimicrobial test. Ahmad Umar would like to acknowledge the support of the Ministry of Higher Education, Kingdom of Saudi Arabia through a grant (PCSED-001-11) under the Promising Centre for Sensors and Electronic Devices (PCSED) at Najran University, Kingdom of Saudi Arabia.

References

[1] D.W. Kolpin, E.T. Furlong, M. Meyer, E.M. Thurman, S.D. Zaugg, L.B. Barber and H.A.T. Buxton, Environ. Sci. Technol, 2002, 36, 1202-1211.

[2] Q. He, J. Liu, C. Huang and W. Wu, Sci. Adv. Mater, 2014, 6, 366-376.

[3] S. Xu, D. D. Sun, J. Nanosci. Nanotechnol. 2013, 13, 6866-6871

[4] D. Ma, T. Wu, J. Zhang, M. Lin, W. Mai, S. Tan, W. Xue and X. Cai, Sci. Adv. Mater, 2013. 5, 1400-1409.

[5] H. Seo, C. M. Elliott, S. G. Ansari, J. Nanosci. Nanotechnol. 2012, 12, 6996-7001

[6] J. Lee, J.-K. Lee, B. H. Park, A. Busnaina, H. Y. Lee, J. Nanosci. Nanotechnol. 2013, 13, 6983-6987

[7] L. Kőrösi, D. Dömötör, S. Beke, M. Prato, A. Scarpellini, K. Meczker, G. Schneider, T. Kovács, Á. Kovács and S. Papp Sci. Adv. Mater, 2013, 5, 1184-1192.

[8] X. Cheng, G. Pan, X. Yu, T. Zheng, A. Umar, Q. Wang, J. Nanosci. Nanotechnol. 2013, 13, 5580-5585

[9] H. Kim, K. Lee, J. Nanosci. Nanotechnol. 2013, 13, 5597-5600

[10] H. Feng, M.-H. Zhang, L. E. Yu, J. Nanosci. Nanotechnol. 13, 4981-4989 (2013)

[11] R. Rohini, Y.T. Chen, R.T.W. Huang, G.H. Lin and I.J. B. Lin, Sci. Adv. Mater, 2013, 5, 216-226.

[12] S. K. Kansal, Mani, H. Kumar, Ahmad Umar, W. Deng, J. Nanosci. Nanotechnol. 2013, 13, 4172-4177

[13] R. S. Hyam, J. Lee, E. Cho, J. Khim, H. Lee, J. Nanosci. Nanotechnol. 2012, 12, 8908-8912

[14] S. G. Ansari, L. Bhayana, Ahmad Umar, A. Al-Hajry, S. S. Al-Deyab, Z. A. Ansari, J. Nanosci. Nanotechnol. 2012, 12, 7860-7868

[15] C.G. Daughton and T.A. Ternes, Environ. Health Perspect, 1999, 107, 907-938.

[16] T. Paul, M.C. Dodd and T.J. Strathmann, Water Res, 2010, 44, 3121-3132.

[17] D. Nasuhoglu, A. Rodayan, D. Berk and V. Yargeau, Chem. Eng. J, 2012, 189-190, 41-48.

[18] M. Sturini, A. Speltini, F. Maraschi, A. Profumo, L. Pretali, E.A. Irastorza, E. Fasani and A. Albini, Appl. Catal. B: Environ, 2012, 119-120, 32-39.

[19] R. Andreozzi, M. Canterino, R. Marotta and N. Paxeus, J. Hazard Mater, 2005, 122, 243-250.

[20] V. Yargeau and C. Leclair, Water Sci. Tech, 2007, 55, 321-326.

[21] V. Yargeau and C. Leclair, Ozone Sci. Eng, 2008, 30, 175-188.

[22] O. González, C. Sans and S. Esplugas, J. Hazard Mater, 2007, 146, 459–464.

[23] R. Andreozzi, V. Caprio, R. Marotta and A. Radovnikovic, J. Hazard Mater, 2003, 103, 233-246.

[24] T.E. Doll and F.H. Frimmel, Chemosphere, 2003, 52, 1757–1769.

[25] R. Palominos, J. Freer, M.A. Mondaca and H.D. Mansilla, J. Photochem. Photobiol. A, 2008, 193, 139–145.

[26] L. Rizzo, S. Meric, D. Kassinos, M. Guida, F. Russo and V. Belgiorno, Water Res, 2009, 43, 979–988.

[27] N.H. Ince and G. Tezcanli, Dyes and Pigments, 2011, 49, 145–153.

[28] S.S. Arbuj, N. Rumale, A. Pokle, J.D. Ambekar, S.B. Rane, U.P. Mulik and D.P. Amalnerkar, Sci. Adv. Mater, 2014, 6, 269-275.

[29] S. Liu, G. Wang, Y. Li and L. Meng, Sci. Adv. Mater, 2014, 6, 361-365.

[30] S.K. Kansal and Prerna, Energy Environ. Focus, 2013, 2, 203-207.

[31] B. Wang, C. Li, W. Wang, J. Zhang, H. Cui, J. Zhai and Q Li, Sci. Adv. Mater, 2013, 5, 1877-1885.

[32] P.S. Badgujar, S.S. Arbuj, J.M. Mali, S.B. Rane and U.P. Mulik, J. Nanoeng. Nanomanuf, 2014, 4, 65-70.

[33] L. Tian, C. Gong, J. Liu, L. Ye and L. Zan, Sci. Adv. Mater, 2013, 5, 1627-1632.

[34] N. A. Mir, A. Khan, K. Umar and M. Muneer, Energy Environ. Focus, 2013, 2, 208-216.

[35] J.X. Kang, T.W. Chen, D.P. Meng, D.F. Zhang, L. Zheng and L. Guo, Sci. Adv. Mater, 2013, 5, 1633-1641.

[36] L. Li, M.A. Gondal, J. Sun, K. Shen and X. Chang, Energy Environ. Focus 2, 2013, 188-194.

[37] M. Liu, H. Wang, C. Yan and John Bell, Mater. Focus 1, 2012, 136-141.

[38] M. A. Gondal, M. A. Dastageer, S. G. Rashid, S. M. Zubair, M. A. Ali, D. H. Anjum, J. H. Lienhard, G. H. McKinley and K. Varanasi, Sci. Adv. Mater, 2013, 5, 2007-2014.

[39] R. K. Soni and M. P. Navas, J. Nanoeng. Nanomanuf, 2013, 3, 341-347.

[40] M. Wang, Y. Gao, L. Dai, C. Cao, Z. Chen and X. Guo, Sci. Adv. Mater, 2013, 5, 1867-1876.

[41] S.S. Arbuj, R.R. Hawaldar, U.P. Mulik and D.P. Amalnerkar, J. Nanoeng. Nanomanuf, 2013, 3, 79-83

[42] J. Han, Y. Liu, N. Singhal, L. Wang and W. Gao, Chem. Engg. J, 2012, 213, 150–162.

[43] S.K. Kansal, M. Singh and D. Sud, Ind. J. Chem. Tech, 2007, 14, 145-153.

[44] S.K. Kansal, A.H. Ali, S. Kapoor and D.W. Bahnemann, Sep Purif Technol, 2011, 80, 125–130.

[45] M. Q. Yang and Y. J. Xu, Phys. Chem. Chem. Phys., 2013, 15, 19102–19118

[46] Y. Zhang, Z. R. Tang, X. Fu, and Y. J. Xu, ACS Nano, 2010, 4, 7303-7314

[47] N. Zhang, Y. Zhang and Y. J. Xu, Nanoscale, 2012, 4, 5792-5813.

[48] N. Zhang, S. Li and Y. J. Xu, Nanoscale, 2012, 4, 2227-2238.

[49] Y. Chen, K.S. Kang, K.H. Yoo, N. Jyoti and J. Kim, J. Phy. Chem. C, 2009, 113, 19753-19755.

[50] H. Li, K. Zheng, Y. Sheng, Y. Song, H. Zhang , J. Huang, Q. Huo and H. Zou, Opt. & Laser Tech, 2009, 49, 33-37.

[51] J. Liqiang, S. Xiaojun, X. Baifu, W. Baiqi, C. Weimin and F. Hongganga, J. Solid State Chem, 2004, 177, 3375–3382.

[52] H. Bai, Z. Liu and D. D. Sun, J. Mater. Chem., 2012, 22, 18801-18807

[53] C. Yu and J. C. Yu, Catal. Lett., 2009, 129, 462–470

[54] D. Wang, L. Xiao, Q. Luo, X. Li, J. An and Y. Duan, J. Hazard. Mater, 2011, 192, 150-159.

[55] S. Yodyingyong, C. Sae-Kung, B. Panijpan, W. Triampo and D. Triampo, Bull. Chem. Soc. Ethiop, 2011, 25, 263-272.

[56] J. Godnjavec, B. Znoj, J. Vince, M. Steinbucher, A. Znidarsic and P. Venturini, Mater. Technol, 2012, 46, 19-24.

[57] N. Daneshvar, D. Salari and A.R. Khataee, J. Photochem. Photobiol. A Chem, 2003, 157,111–116.

[58] D.D. Dionysiou, M.T. Suidan, E. Bekou, I. Baudin and J.M. Laîné, Appl. Catal. B Environ, 2000, 26, 153–171.

[59] M. Shao, X. Xu, J. Huang, Q. Zhang, and L. Ma, Sci. Adv. Mater, 2013, 5, 962-981.

[60] A.L Giraldo, G.A. Penuela, R.A. Torres-Palma, N.J. Pino, R.A. Palominos and H.D. Mansilla, Water Res, 2010, 44, 5158-5167.

Figure Captions

Figure 1. (a) Typical TEM and (b) HRTEM images; (c) EDS spectrum and (d) XRD pattern of as-prepared TiO_2 nanoparticles

Figure 2. Typical (a)FTIR spectrum and (b) room-temperature photoluminescence (PL) spectrum of as-prepared TiO_2 nanoparticles

Figure 3. DSC-TGA analysis of prepared of as-prepared TiO_2 nanoparticles

Figure 4. (a) Time dependent UV-Vis absorption spectra for Levofloxacin (LEVO; conc = 25 mg/L, pH= 6, catalyst dose= 1g/L), (b) extent of decomposition (C/C_0) of LEVO with respect to time intervals.

Figure 5. (a) Comparison of degradation efficiencies for different photocatalysts (as prepared TiO_2 nanoparticles and commercially available TiO_2 (PC-50) and P25 towards LEVO; (b) Percentage degradation rates observed Recyclability

Figure 6. Schematic illustration of photocatalysis reaction for the photocatalytic degradation of Levofloxacin using prepared TiO_2 nanoparticles.

Figure 7. Antibacterial activity measured as inhibition zone diameter during photocatalysis

Figures

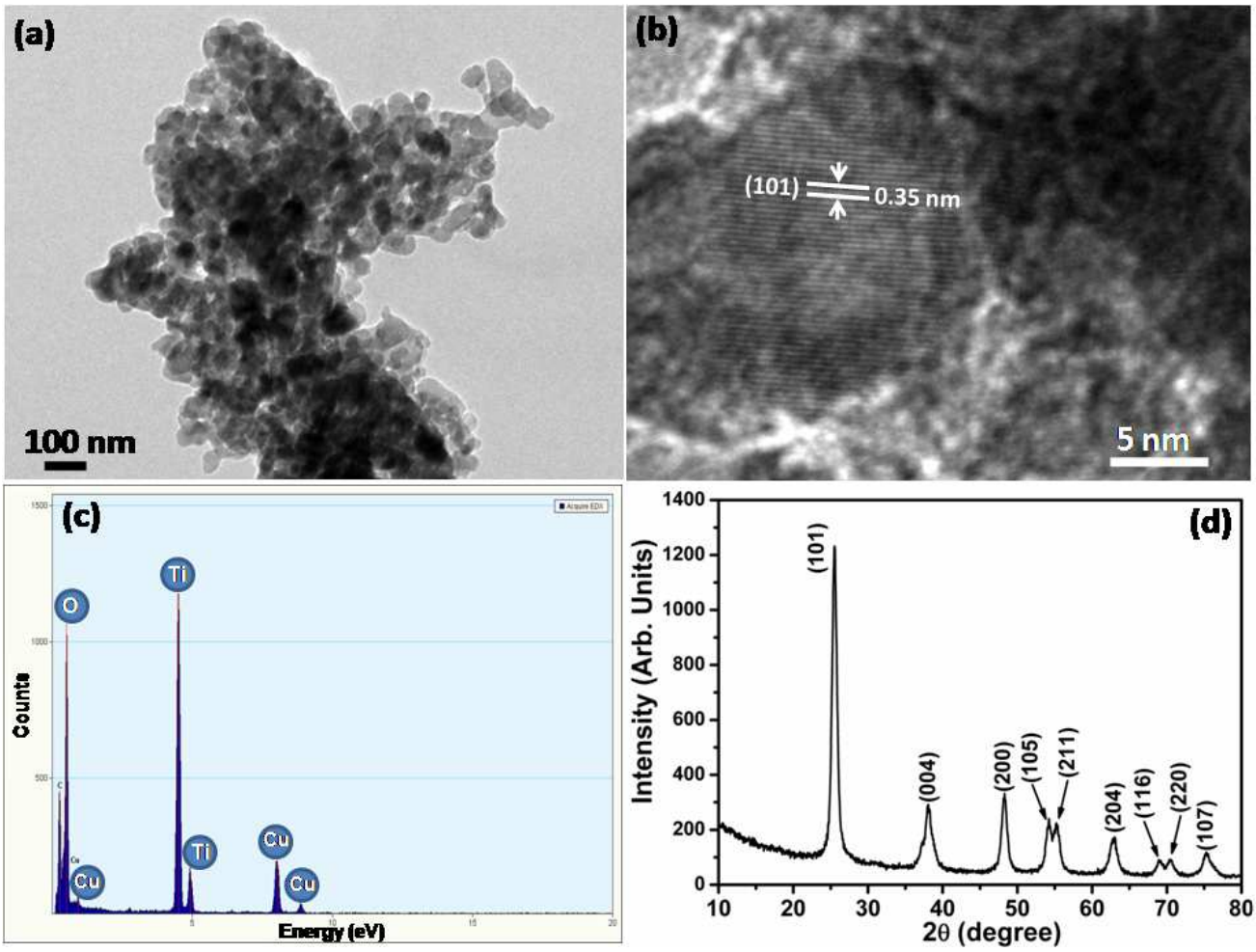

Figure-1

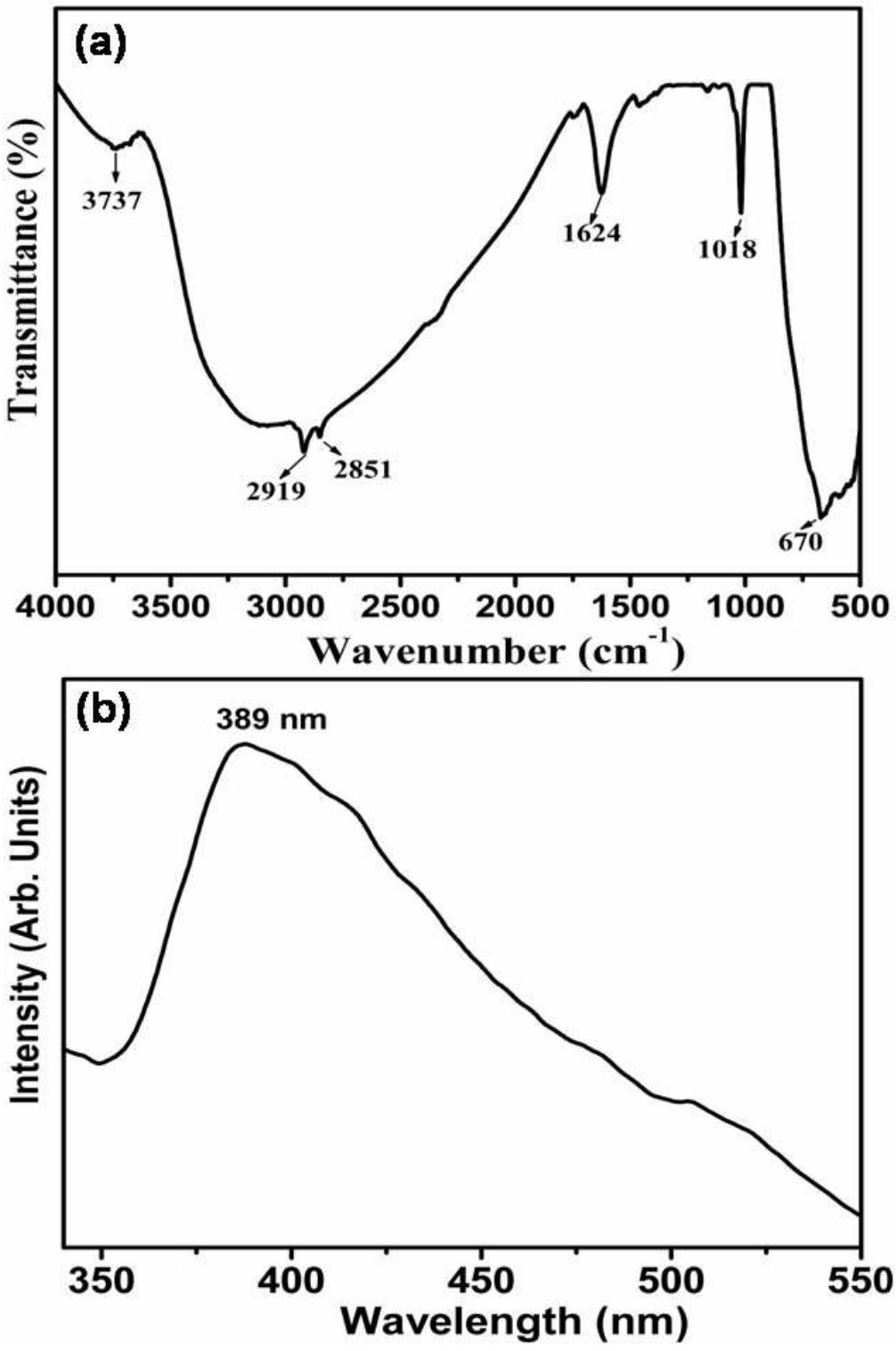

Figure-2

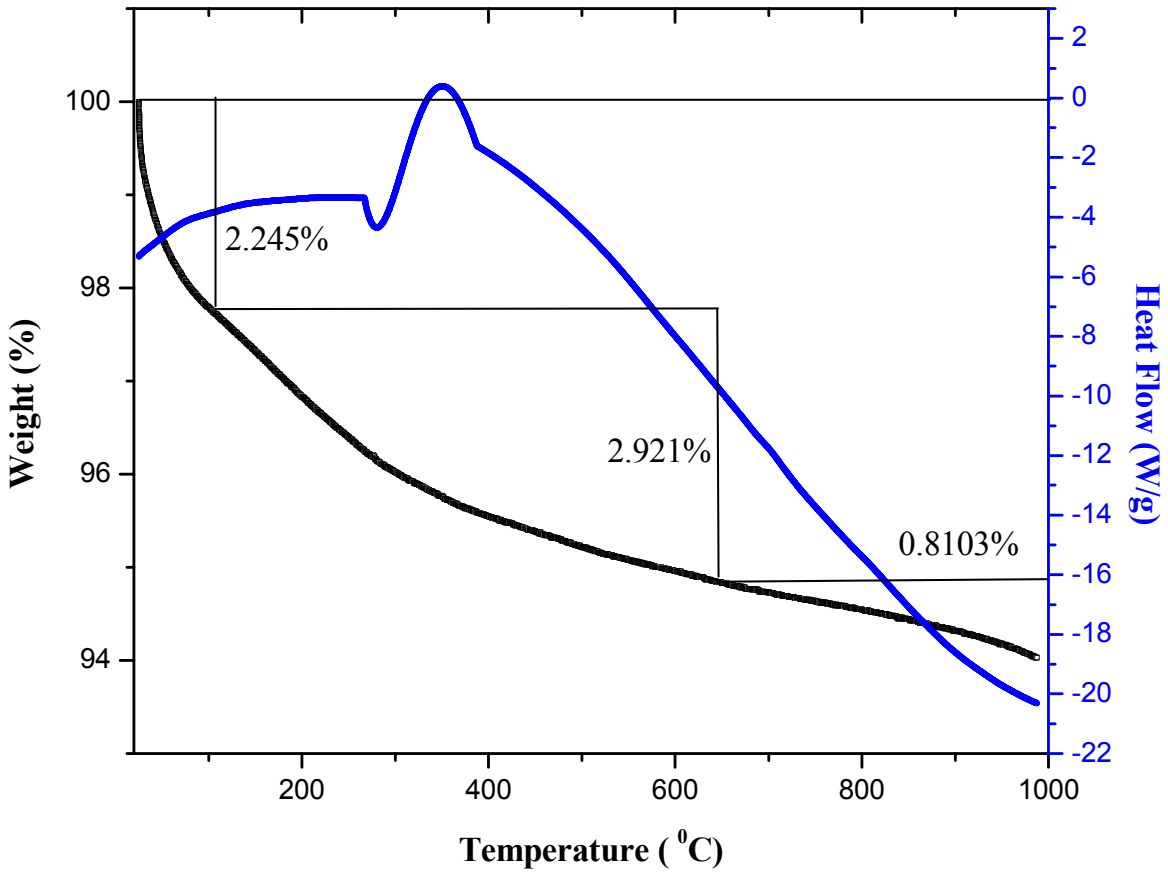

Figure-3

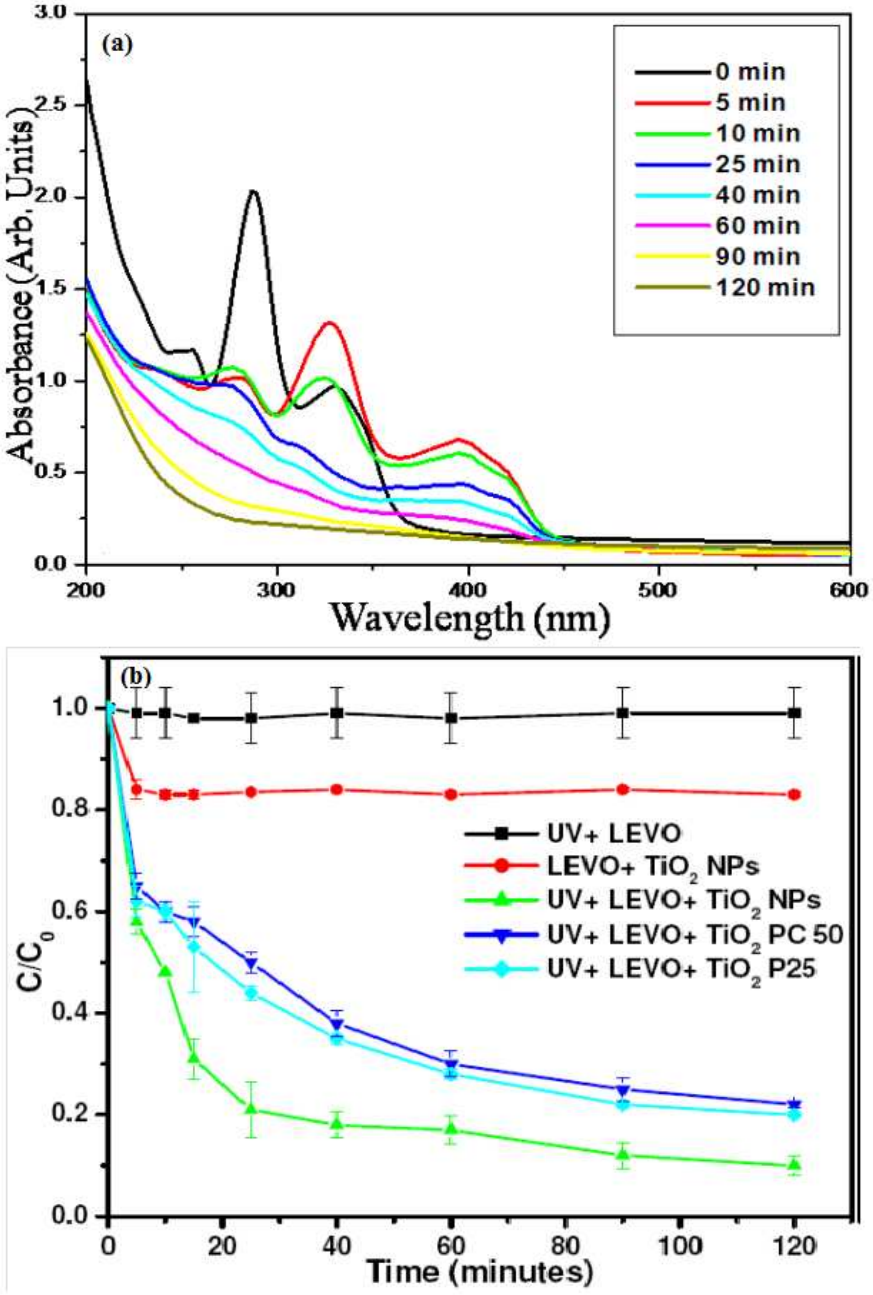

Figure-4

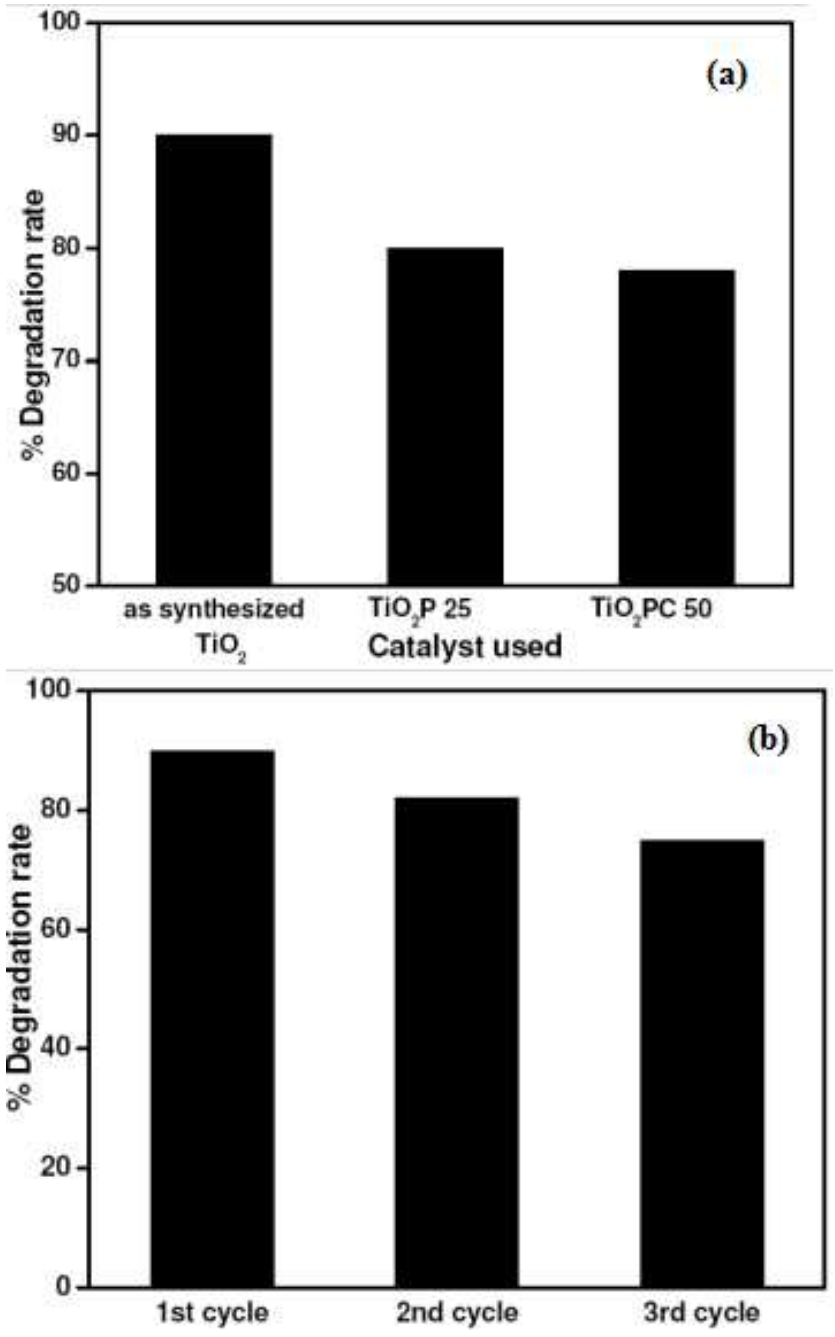

Figure-5

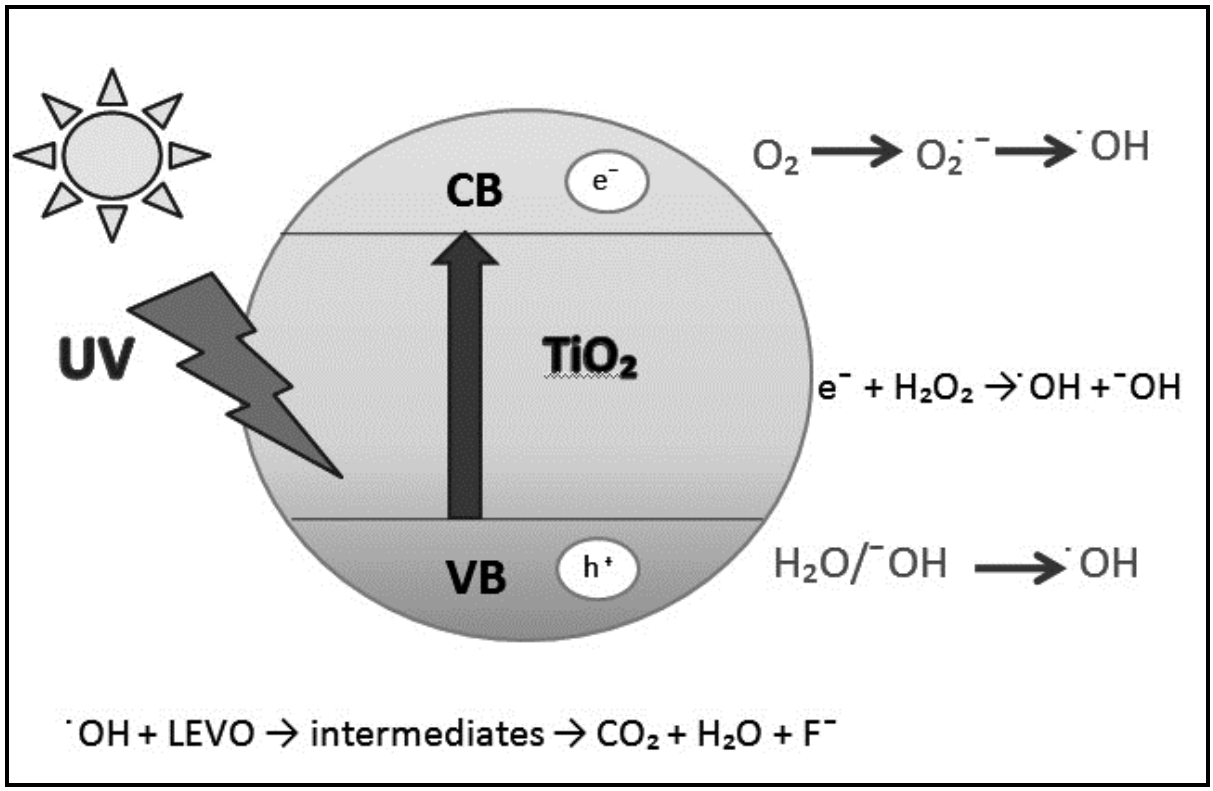

Figure-6

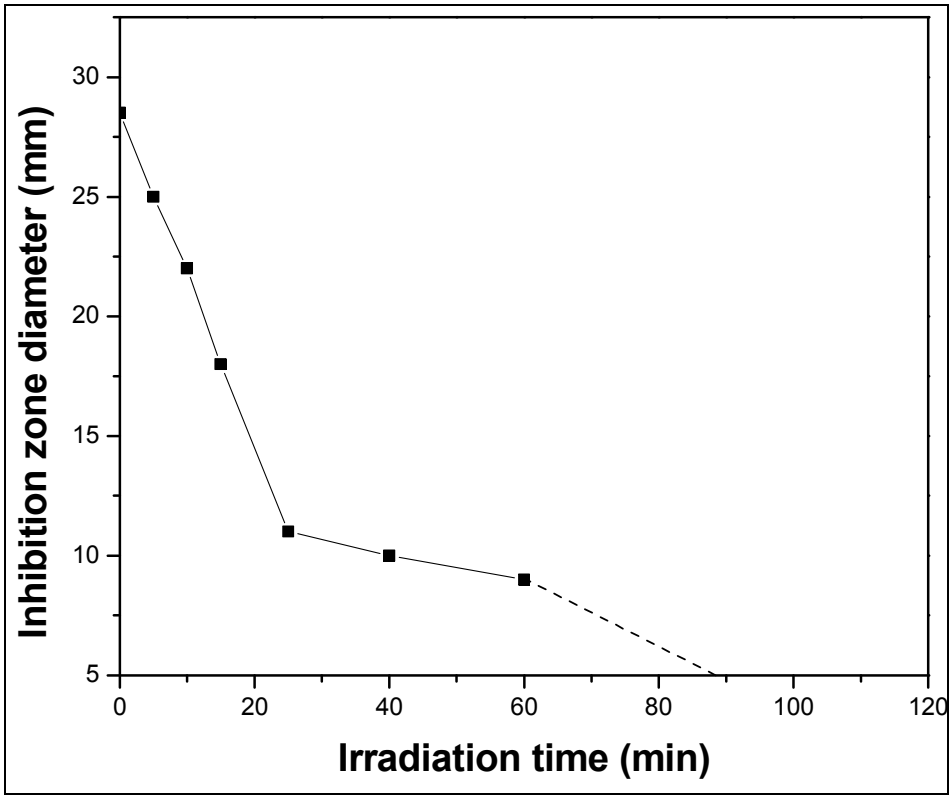

Figure-7